Distribution Agreement

In presenting this thesis as a partial fulfillment of the requirements for a degree from Emory University, I hereby grant to Emory University and its agents the non-exclusive license to archive, make accessible, and display my thesis in whole or in part in all forms of media, now or hereafter now, including display on the World Wide Web. I understand that I may select some access restrictions as part of the online submission of this thesis. I retain all ownership rights to the copyright of the thesis. I also retain the right to use in future works (such as articles or books) all or part of this thesis.

Phillip M. Rauscher April 16, 2013

Effect of Adjacent Rubbery Layers of the Physical Aging of Polymer Glasses

By

Phillip M. Rauscher

Connie B. Roth
Adviser

Department of Physics

Connie B. Roth
Adviser

Eric R. Weeks
Committee Member

Michael F. McCormick
Committee Member

2013

Effect of Adjacent Rubbery Layers on the Physical Aging of Polymer Glasses

By

Phillip M. Rauscher

Connie B. Roth
Adviser

An abstract of
a thesis submitted to the Faculty of Emory College of Arts and Sciences
of Emory University in partial fulfillment
of the requirements of the degree of
Bachelor of Sciences with Honors

Department of Physics

2013

Abstract

Effect of Adjacent Rubbery Layers on the Physical Aging of Polymer Glasses

By Phillip M. Rauscher

Upon cooling through their glass transition temperature (T_g), polymers form non-equilibrium solids and subsequently undergo physical aging. I developed a method of measuring the physical aging rate of thin polystyrene (PS, T_g = 373 K) films atop poly(*n*-butyl methacrylate) (PnBMA, T_g = 299 K) layers at aging temperatures between the two polymer T_gs in order to investigate the effect of a glassy/rubbery interface on structural relaxation in confined glassy polymer systems. To accomplish this, I devised a new ellipsometry protocol and data analysis method, expanding off a previous method developed in the Roth laboratory for characterizing the physical aging rate of single layer films. In order to interpret my results, I also used fluorescence spectroscopy to measure the T_g of the PS layer in the bilayer morphology. Despite very large reductions in PS T_g in the bilayer system no reductions in physical aging rate are observed, in strong contrast to results from single layers, suggesting the presence of some undefined mechanism stemming from the glassy/rubbery interface.

Effect of Adjacent Rubbery Layers on the Physical Aging of Polymer Glasses

By

Phillip M. Rauscher

Connie B. Roth
Adviser

A thesis submitted to the Faculty of Emory College of Arts and Sciences
of Emory University in partial fulfillment
of the requirements of the degree of
Bachelor of Sciences with Honors

Department of Physics

2013

Acknowledgements

I gratefully acknowledge Eric Weeks and Michael McCormick for taking time out of their schedules to serve on my committee. Furthermore, I thankfully acknowledge all members of the Roth laboratory, especially Laura Gray, Justin Pye, and Roman Baglay. I also extend my thanks to family, friends, the Alpha Tau Omega fraternity, Dooley Noted A Cappella, and Rachel DelGaudio for their support. Above all, I thank my adviser Connie Roth. This work would not exist were it not for her outstanding mentorship.

Table of Contents

List of Figures

Introduction

Polymers and Advanced Applications

Polymers (very long chains of linked monomers) are ubiquitous. Simply listing the names of several common synthetic and biological polymers – Styrofoam, Nylon, Plexiglas, DNA, etc. – more than adequately illustrates the impact of these molecules on our lives. And the applications are ever-growing, especially as our technology continues to shrink. Advances in polymer manufacturing have resulted in nanoscale domain sizes, allowing for the integration of polymers into modern nanotechnology and nanoscience. For example, applications of certain layered polymeric systems range from high-performance optical devices[1] to effective gas separation membranes.[2] Such multilayer systems can be assembled with up to thousands of alternating layers.[3,4] With the emergence of these new nanolayered polymer systems, it is increasingly important to develop an understanding of their properties as they are affected by nanoconfinement as well as the presence of interfacial regions unique to these morphologies.

Glassy Behavior and Physical Aging

Polymers rarely form equilibrium solids upon cooling. Rather, they form non-equilibrium glasses when quickly cooled through a certain temperature (a material property), aptly termed the glass transition temperature (T_g). The glass transition is represented schematically on a volume vs. temperature plot in **Figure 1**. This transition and the associated behaviors are still poorly understood physical phenomena, lacking an adequate theoretical description. It is important to note that the glass transition is not a true phase transition (e.g. liquid to gas transition) but is referred to as a kinetic transition. The material thermally contracts too quickly for it to rearrange into an equilibrium

configuration and the entire sample becomes energetically frustrated. Hence, if a sample could be cooled infinitely slowly (or at least more slowly than a laboratory time scale will allow e.g. $1°C/10^9$ years), there is debate whether the material would ever fall out of equilibrium, remaining energetically comparable to a super-cooled liquid, or if a true thermodynamic phase transition would eventually intervene forming a so-called "ideal glass." Heating the glass to above T_g allows it to relax back into equilibrium, reforming a rubbery, liquid-like substance. Thus, annealing above T_g for an extended period of time is a common method for "resetting" the thermal history of a glass.

Once a sample of polymer is in a glassy configuration, it experiences a driving force towards equilibrium, giving off excess enthalpy by rearranging into a lower-energy

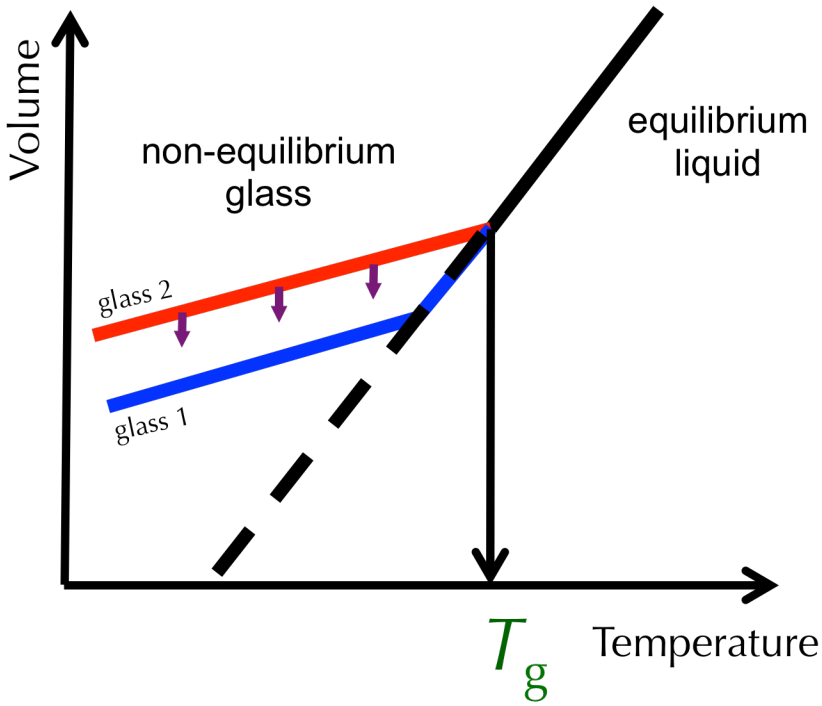

Figure 1. A schematic representation of basic glassy behavior. As the equilibrium liquid-like polymer (solid black line) is cooled, it falls out of equilibrium at T_g and becomes a glass (red line). The glass then undergoes physical aging (purple arrows) into a lower-energy glass (blue line) which is energetically closer to equilibrium (dashed black line).

state. This process, called physical aging, is also shown schematically by the purple arrows in **Figure 1** and results in volume contractions. These volume reductions are often much less than 1%, but can cause large variations in other material properties. For instance, thin films of polysulfone, a stiff backboned polymer used for gas separation membranes, can lose more than 50% of their oxygen permeability over a period of six months due to physical aging.[2] It is important to note that while glassy behavior is common in polymers, it is not unique to them. Glasses can be formed naturally (e.g. amber, obsidian) as well as with small molecules (e.g. toluene, indomethacin) and all of these glasses experience physical aging.

Goal of Thesis

The main focus of this thesis is to develop a method of measuring the physical aging rate polystyrene (PS, T_g = 373K, 100°C) films atop poly(*n*-butyl methacrylate) (PnBMA, T_g = 299K, 26°C) at aging temperatures between the two polymer T_gs in order to investigate the effect of a glassy/rubbery interface on structural relaxation in confined glassy polymer systems. To accomplish this, I devised a new ellipsometry protocol and data analysis method, expanding off of a previous method developed in the Roth lab for characterizing the physical aging rate of single layer films.[5,6] In order to interpret my results, I also used fluorescence spectroscopy to measure the T_g of the PS layer within the bilayer morphology.

Background

Measurement of T_g using Fluorescence Spectroscopy

There are several methods of measuring T_g in polymer systems. Fluorescence spectroscopy is among the most useful for measuring T_g in PS films.[7] Pyrene, a fluorescent dye sensitive to the local density of the polymer is either doped into the sample or attached chemically to the polymer chain during synthesis. When the sample is excited with UV light, the dye absorbs a photon and enters an excited state. It then relaxes into a slightly lower energy state via vibrational relaxations, and then emits a lower-energy photon as it returns to the ground state. Instead of fluorescing, the molecule can also return to the ground states through other mechanisms, termed "non-radiative decay." This process is shown schematically in **Figure 2**. The relative

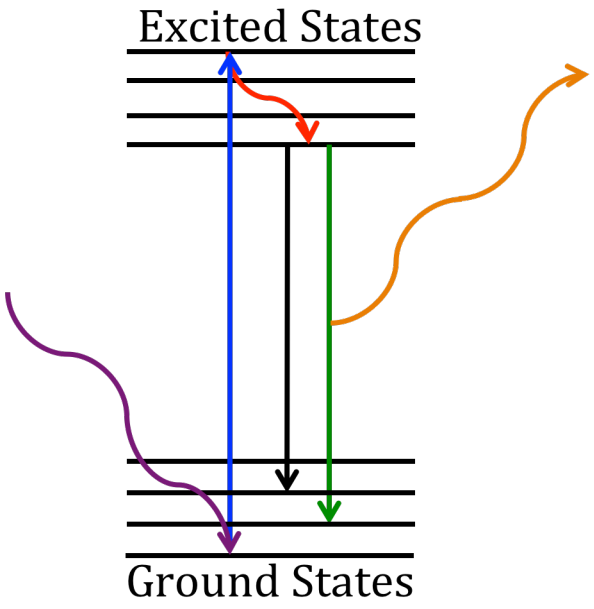

Figure 2. A schematic representation of the fluorescence process. The fluorophore absorbs a high-energy photon (purple arrow) and enters an excited state (blue arrow). Small vibrational relaxations (red arrow) occur followed by either non-radiative decay (black arrow) or emission (green arrow) of a lower-energy photon (orange arrow). The various photon wavelengths associated with relaxations into various ground states determines the shape of the fluorophore's emission spectrum.

incidence of relaxations into various levels of the ground states determines the unique shape of a given fluorophore spectrum. The emission intensity of the pyrene dye labeled to PS used in this study is shown in **Figure 3** as a function of wavelength. The pyrene dye is sensitive to the local polymer density;[7] lower temperature and less mobile polymer surrounding the dye allows for less non-radiative decay and therefore increased fluorescence, mirroring the changes in density. As the polymer is cooled, its density increases, with a change in rate of increase occurring at T_g. Therefore, a change in slope of normalized integrated pyrene fluorescence intensity versus temperature also occurs at T_g, as shown in **Figure 4**. This method is useful since careful placement of fluorescent dyes can allow researchers to probe the T_g of specific locations within multilayer polymer films.[7-9]

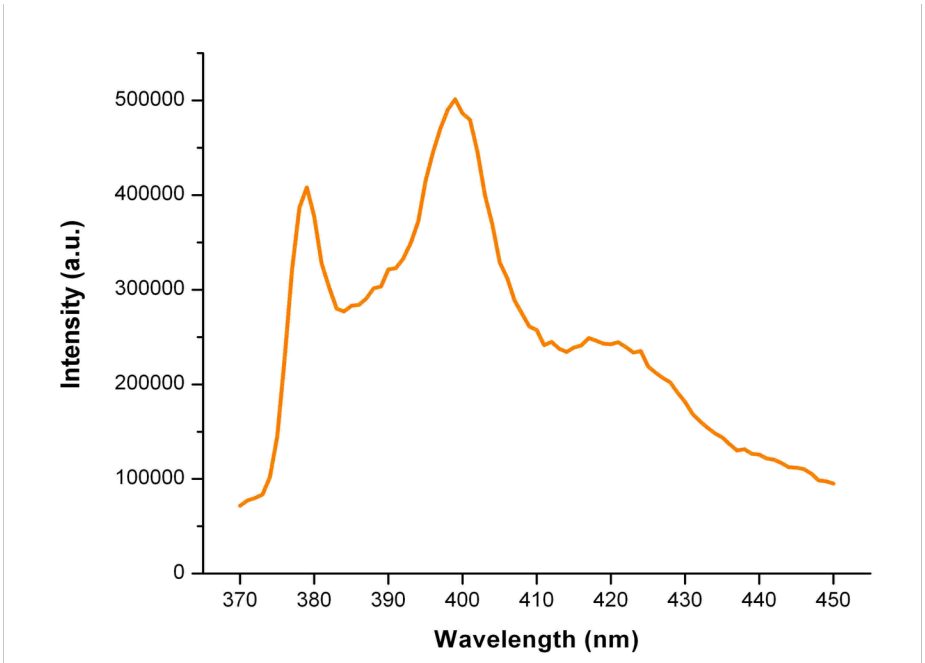

Figure 3. Fluorescence emission spectrum of pyrene-labeled PS from a ~100 nm thick film on quartz. The particular 1-pyrenyl butyl methacrylate dye labeled to PS is shown in **Figure 11c**.

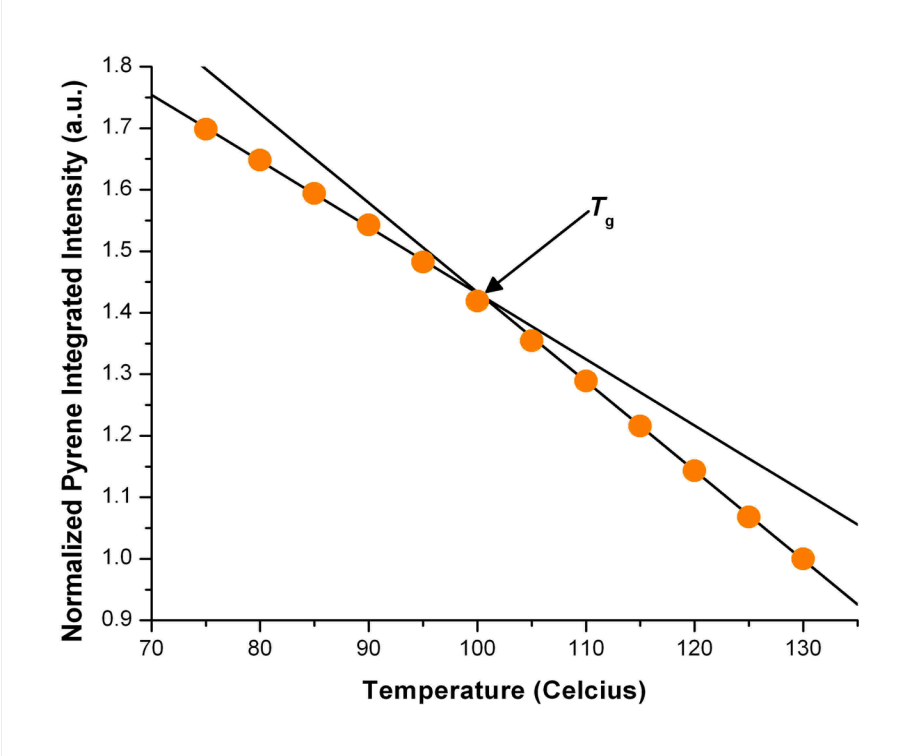

Figure 4. Normalized integrated fluorescence intensity of a ~100 nm thick pyrene-labeled PS film as a function of temperature. Data collected using the same measurement protocol described in ref. 7. The film was cooled from 130°C to 75°C and the fluorescence spectrum was measured and integrated every 5°C. The T_g of the polymer film occurs where a change in slope is observed. This is determined quantitatively by finding the intersection of the two lines, which are fits to the first 5 and last 5 data points.

Measurement of Physical Aging by Ellipsometry

Ellipsometry, an advanced optical technique, is an excellent method of measuring the thickness of thin films. A thin polymer film (n ~ 1.5) is placed on a material with a very different index of refraction (usually a silicon wafer with n ~ 3.8) to generate good optical contrast. A beam of elliptically polarized light (400 nm-1000 nm in wavelength) is sent into the sample. The beam reflects and refracts within the film and the beam reflected from the sample is analyzed by a detector to measure the change in polarization (i.e. the ellipsometric angles Ψ and Δ) at various wavelengths. These data can then be

used to determine the total reflection coefficients $\tilde{R}_p$ and $\tilde{R}_s$ by **Equation 1**, the fundamental equation of ellipsometry:[10]

$$\frac{\tilde{R}_p}{\tilde{R}_s} = \tan(\Psi)e^{i\Delta} \tag{1}$$

These coefficients can be fit to a Cauchy model for refractive index n as function of wavelength λ and film thickness of transparent materials, shown in **Equation 2** (where A_n, B_n, etc are fitting parameters):

$$n(\lambda) \approx A_n + \frac{B_n}{\lambda^2} + \frac{C_n}{\lambda^4} + \ldots \tag{2}$$

This method of measuring film thickness is sensitive to changes in thickness of a tenth of an Angstrom, which allows for physical aging measurements in ultrathin polymer films despite the very small changes in volume associated with physical aging (<1%).[5,6]

In the Roth lab, Baker et al. recently developed a streamlined ellipsometry procedure for measuring physical aging in ultrathin PS films.[5] Rather than age the samples in an oven over an extended period of time and take measurements every few days or weeks (as is common for other types of aging measurements), the physical aging was measured *in situ*. The samples (PS films of thickness 2430 nm ± 120 nm) were placed on the ellipsometer hot stage at the aging temperature and measurements were taken, averaging over a 30 second period, every 5 minutes for up to 24 hours. Normalized film thickness as a function of time is shown for one of these samples in **Figure 5**. They demonstrated that reliable aging rates can be obtained by analyzing the index of refraction, Lorentz-Lorenz parameter, and film thickness.[5] For simplicity, they chose to use **Equation 3**:

$$\beta = -\left[\frac{\partial h/h_o}{\partial \log(t_a)}\right]_{P,T} \tag{3}$$

where the physical aging rate β is the slope of the normalized film thickness, h/h_0, versus the logarithm of the aging time, $\log(t_a)$, at constant pressure P and temperature T. Furthermore, they demonstrated that aging rates at 65°C could be reliably measured for PS with only 6 hours of aging time. It should be noted that this method measures the *average* physical aging rate of the entire film. This thesis will expand on this streamlined method to reliably measure the physical aging rate of glassy PS on top of rubbery PnBMA.

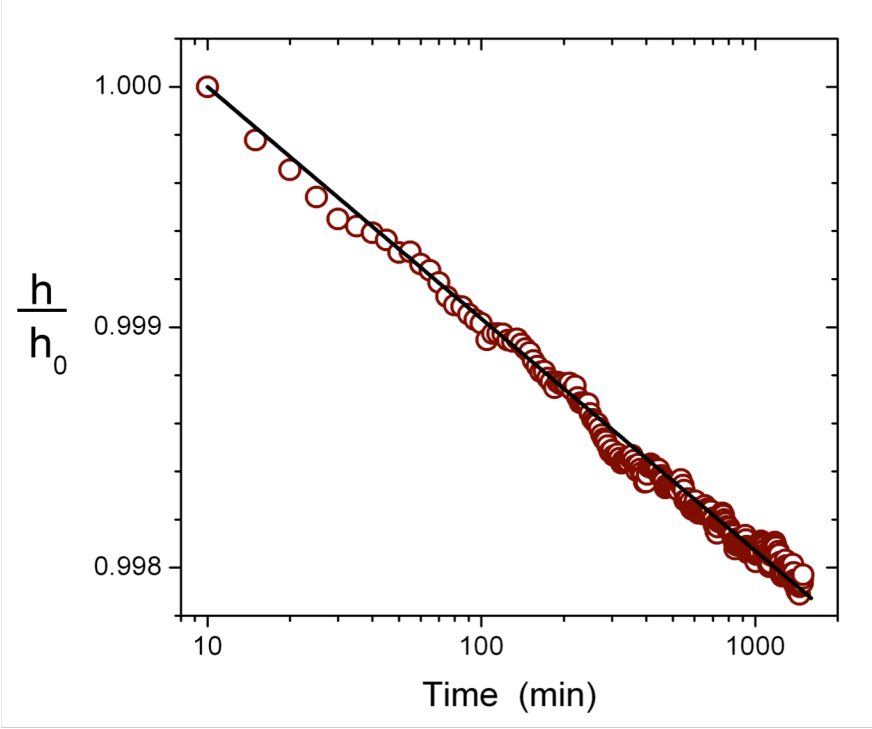

Figure 5. Normalized film thickness of a bulk PS film (~2400 nm) as function of log(time). The physical aging rate, β, is defined as the slope of the best-fit line (**Equation 3**). [Data taken from ref. 5]

Polymer Glasses in Confinement

When polymer materials are placed in confined systems, glassy behaviors deviate significantly from bulk. These effects have been most studied in thin, supported polymer films of thickness <100 nm. In these systems, the glassy polymer has two interfaces as shown in **Figure 6**: one at the substrate (usually a silicon wafer or glass) and another at the free surface, both of which can noticeably affect the glass transition and physical aging of the material at small length scales. For instance, it has been shown that ultrathin polystyrene (PS) films exhibit a decrease in average T_g at thicknesses <60 nm[11,12] as shown in **Figure 7**.

This confinement effect has been attributed to enhanced mobility at the free surface causing a gradient of dynamics in the film. If the polymer is very mobile at a particular depth within the film (i.e. fast dynamics), then it can remain liquid-like at lower temperatures, causing a lower local T_g and consequently a lower average T_g. Ellison and Torkelson observed just such a gradient in T_g in thin PS films (large T_g reductions at the free surface and bulk T_g deeper in the film) using fluorescence spectroscopy.[7] Conversely, poly(2-vinyl pyridine) has shown an increase in T_g at similar

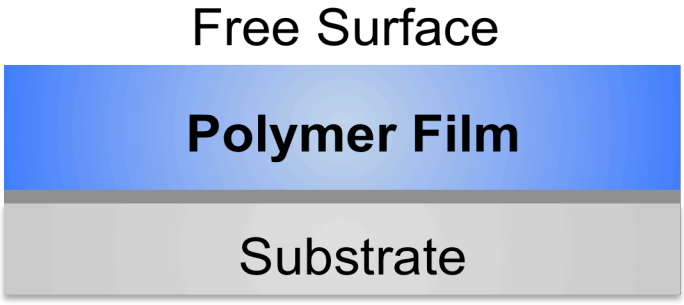

Figure 6. A schematic representation of a supported polymer film. The polymer is fixed to the substrate at the bottom (a silicon wafer with a silicon oxide layer), and exposed to air at the top; these two interfaces can significantly affect the behavior of the polymer.

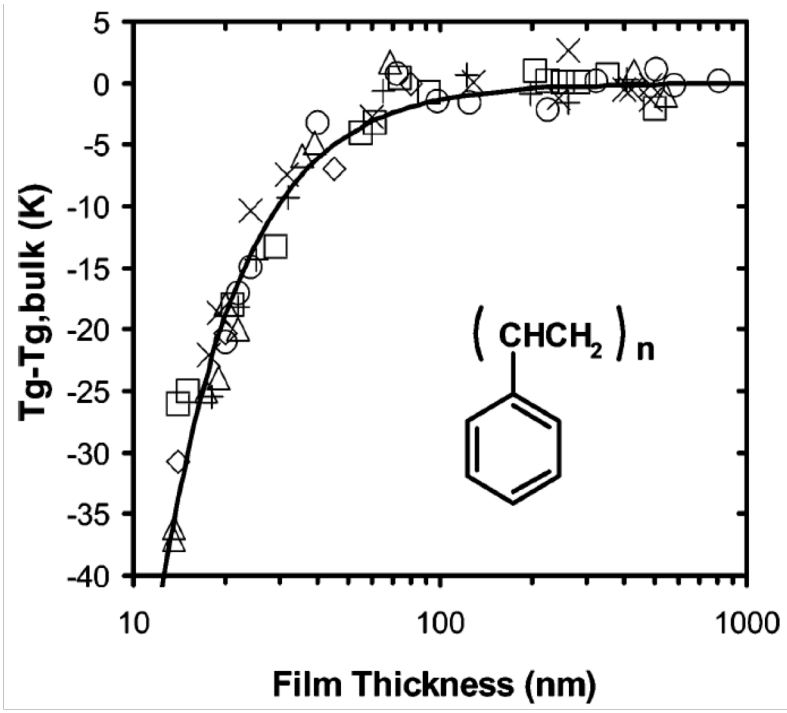

Figure 7. T_g of PS films supported on quartz as a function of film thickness as measured by fluorescence. Significant reductions in T_g in the ultrathin regime are attributed to faster dynamics at the free surface, which reduce the average film T_g measured. [Figure reproduced from ref. 12, with permission].

thicknesses.[9] In this case, it is believed that the free surface effect is outweighed by hydrogen bonding with the substrate (which PS does not have), restricting mobility. Finally, poly(methyl methacrylate) films showed only a small increase in T_g, indicating that effects from the free surface versus the substrate are approximately equal and opposite.[13,14] Clearly, the T_g of an ultrathin polymer film depends a great deal on the kinds of interfaces present in the system.

The gradient in T_g observed in thin PS films by Ellison and Torkelson[7] would result in a gradient in physical aging rate within the films as well. The T_g at the surface of a PS film has been previously estimated to be as low as 27°C,[15] such that at any higher temperature, the free surface is above T_g (in equilibrium) and does not age. Further into the film, bulk T_g is recovered, along with bulk physical aging rate, presumably. For

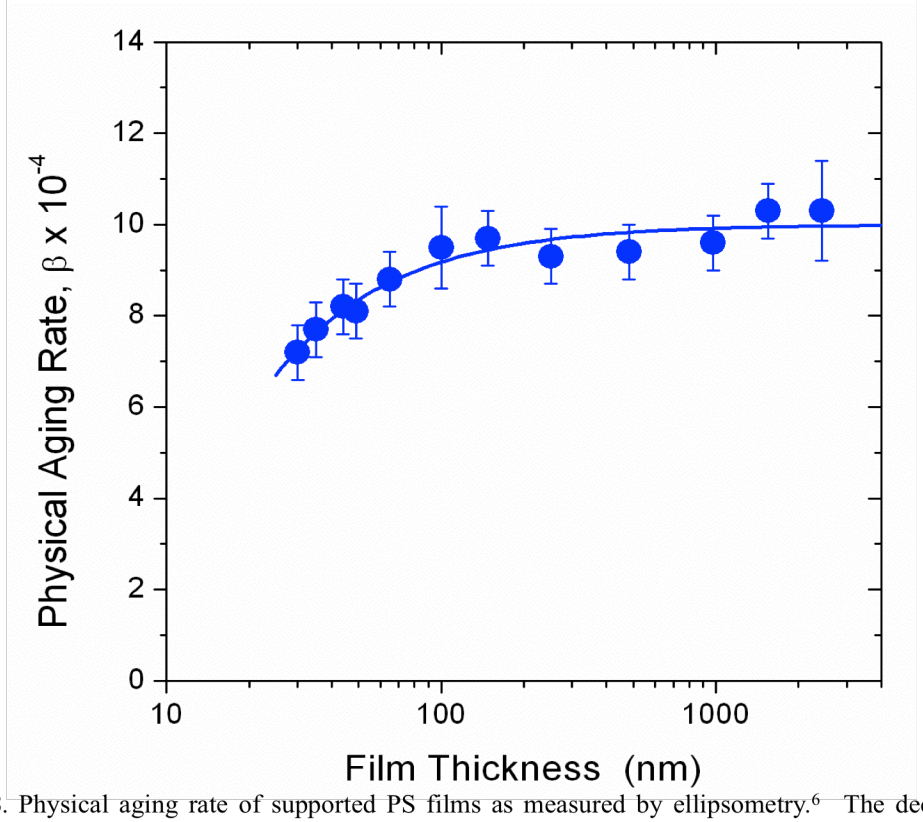

Figure 8. Physical aging rate of supported PS films as measured by ellipsometry.[6] The decrease in aging rate below ~60 nm is linked to the gradient in T_g observed for these same films. T_g is greatly reduced at the free surface (by up to 73°C according to one estimate[15]) and bulk T_g is recovered deeper into the film.[7] Given that the aging temperature of these films is 65°C, Pye et al.[6] assumed that no aging occurs at the free surface and that bulk aging rates are recovered deeper into the film, corresponding to a gradient in dynamics. Therefore, as the total film thickness is reduced, the non-aging region of the film becomes a greater fraction of the total thickness and the average aging rate is lowered. [Data taken from ref. 6].

supported PS films, behavior consistent with this gradient in dynamics is seen in physical aging rates as film thickness is decreased,[6] as shown in **Figure 8**; below 60 nm, these films exhibit reduced physical aging rates as measured by Pye et al.[6] via ellipsometry.

Pye et al.[6] also showed the physical aging rate of 2400 nm thick PS single layers at various temperatures and parametrized the data with a 2nd order polynomial, as shown by the filled circles and upper solid curve in **Figure 9**. The general shape of the thick film's curve can be explained by two competing effects: distance from the equilibrium line and thermal motion. At low aging temperatures, the glass is farther from its equilibrium line (see **Figure 1**), producing a greater driving force for aging. However,

low temperature also implies less thermal energy, which limits the motion of the chain segments and does not allow for rapid physical aging. Conversely, at high temperatures, the chain segments are more mobile due to high thermal energy, but do not have a strong driving force towards equilibrium. It is tempting to think that the reduced aging rates in thin films result simply from a change in distance from T_g due to the T_g reductions in thin films, such that the aging rate vs. temperature curve for a thinner film would simply be shifted to lower temperatures. However, this is *not* the case. Pye et al.[6] showed that the aging rate of ultrathin (29 nm thick) PS films is reduced from the bulk value at *all* aging temperatures, as shown by the open triangles in **Figure 9**. In order to interpret this result, Pye et al.[6] modeled the gradient in aging rate in two ways as shown in **Figure 10**.

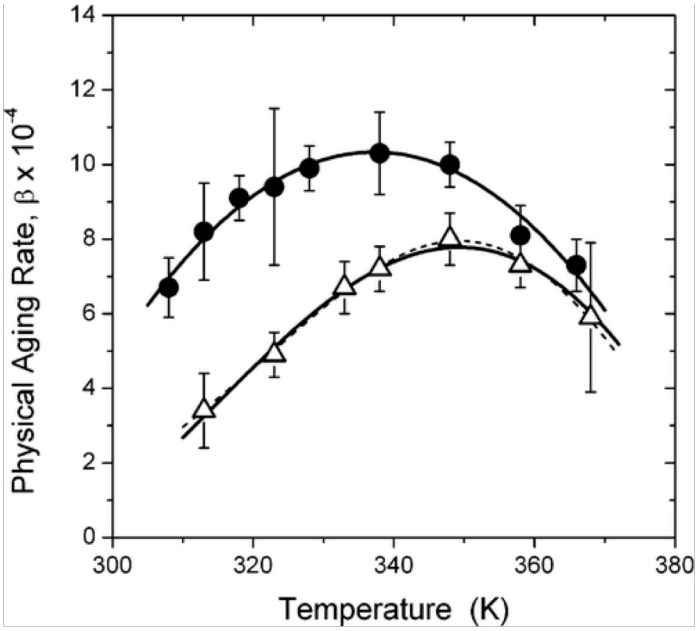

Figure 9. Physical aging rate of 2400 nm thick PS single layers (filled circles) and 29 nm thick PS single layers (open triangles) as a function of aging temperature as determined by **Equation 3**.[6] The 2400 nm bulk data were parametrized with a 2nd order polynomial (upper solid curve) and used in the two layer model (**Equation 4**, lower solid curve) and the gradient model (**Equation 6**, dashed curve) to determine values of $A(T)$ and $\lambda(T)$, respectively. Each data point is an average of 2-6 samples. [Figure reproduced from ref. 6, with permission].

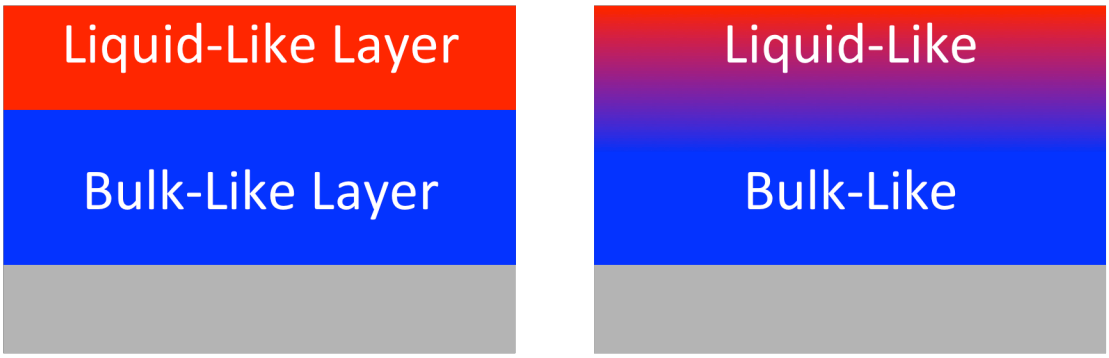

Figure 10. An illustration of the two models used by Pye et al.[6] for physical aging in single-layer PS films. In the two-layer model (left), the surface layer is in equilibrium and experiences no aging while the layer underneath undergoes bulk aging. The thickness of the surface layer is treated as a fitting parameter. The gradient model (right) assumes no aging at the free surface and a single exponential transition to a bulk physical aging rate as the distance from the free surface is increased. The length scale of this exponential is treated as a fitting parameter. Both of these models are based on the idea of a gradient in dynamics stemming from the free surface and are simply two different ways of representing the same phenomenon.

First, a simple two-layer model comprising a liquid-like surface layer (no aging as the surface T_g is reduced to below the aging temperature) and a bulk underlayer (bulk aging rate) was used where the average physical aging rate $\beta(h,T)$ of a film of thickness h at temperature T is given by **Equation 4**:

$$\beta(h,T) = \beta_{Bulk}(T)\left[1 - \frac{A(T)}{h}\right] \tag{4}$$

where $\beta_{Bulk}(T)$ is the physical aging rate of bulk PS and $A(T)$ is the thickness of the liquid-like surface layer. $A(T)$ was used as a fitting parameter to obtain a rudimentary measure of how free surface dynamics could propagate deeper into the film. In the second, presumably more realistic, model, an exponential gradient in dynamics was assumed, with no aging at the free surface transitioning into a bulk aging rate deeper into the film according to a characteristic length scale $\lambda(T)$ (another fitting parameter). Thus, the aging rate at a depth z from the free surface is given by **Equation 5**:

$$\beta(z,T) = \beta_{Bulk}(T)\left[1 - \exp(-z/\lambda(T)\right] \tag{5}$$

The average aging rate of the film is obtained by integrating **Equation 5** over the entire thickness of the film, h, and dividing the result by the film thickness. The result is **Equation 6**:

$$\beta(h,T) = \beta_{Bulk}(T)\left[1 - \frac{\lambda(T)}{h}\left\{1 - \exp\left(-\frac{h}{\lambda(T)}\right)\right\}\right] \tag{6}$$

The length scales $A(T)$ and $\lambda(T)$ were then calculated from **Equation 4** and **Equation 6**, respectively, using the quadratic fit of the 2400 nm thick films (upper solid curve in **Figure 9**) for the $\beta_{Bulk}(T)$ term. In **Figure 9**, the lower solid curve shows **Equation 4** with the resultant values of $A(T)$ and the dashed curve shows **Equation 6** with the resultant values of $\lambda(T)$. Both the two-layer model and the gradient model fit the data well and provide meaningful measures of how far into a film the enhanced free surface dynamics propagate. The length scales $A(T)$ and $\lambda(T)$ both show an increase in length scale as temperature is decreased. Similar results have been observed for two-layer models describing T_g reductions in thin films, strongly suggesting a link between this behavior and cooperative dynamics and T_g.[6,15]

Physical Aging in Glassy/Rubbery Systems

Due to exciting new technological applications, attention in the scientific community has shifted towards physical aging of more complex morphologies at the nanoscale, such as the polymer multilayers mentioned earlier. Glassy/rubbery multilayers are of particular interest, as they bring together two very different materials at the nanoscale. These materials have no "hard" interface. Rather, there is a region

between the layers in which the rubbery and glassy polymers are mixed together. This "interface" layer can be several nanometers thick for immiscible polymers. For the PS/PnBMA system studied here, the interface has been measured to be 7 nm in width.[16] Given that T_g and physical aging of glassy polymers are very sensitive to the boundary conditions of the material at the nanoscale, we expect the presence of a rubbery layer to significantly perturb the system. Several studies have documented physical aging in various multilayer systems. For instance, Rowe, Freeman, and Paul[2] studied the physical aging of thin films of polysulfone (PSF), a stiff-backboned glassy polymer, by gas permeability coated with rubbery polydimethylsiloxane (PDMS). Ultrathin gas separation membranes are commonly coated with rubbery PDMS to cover pinhole defects. They observed an increase in physical aging rate (compared to bulk) with decreasing glassy layer thickness (down to 20nm thick films) identical to increases previously observed in PSF single layers, suggesting that the rubbery layer may act similar to a free surface.[2]

Additionally, Tant and Wilkes used mechanical properties to study the physical aging of styrene-butadiene-styrene block copolymers as a percentage of glassy content.[17] Block copolymers synthesized from immiscible polymer components are known to segregate into heterogeneous domains, with numerous glassy/rubbery interfaces throughout the sample. With decreasing glassy fraction, which would presumably correspond to smaller glassy domains and therefore more glassy polymer in close contact with the glassy/rubbery interface, they observed an *increase* in physical aging rate. Although they collected no data on copolymers with glassy fraction below 50%, they noted that at 0% the physical aging rate must go to zero (since the sample would be

completely rubbery). Unfortunately, the molecular weight of the copolymer blocks was not given, so no estimate can be made of their domain sizes, limiting any quantitative comparison.

Baer and coworkers have extensively studied polymer systems consisting of alternating layers of immiscible polymers created by multilayer co-extrusion (also called "forced assembly").[3,4,18-20] Using this fabrication technique, alternating layer systems can be created with up to thousands of layers with thicknesses down to 8 nm, at which point a significant fraction of the material is interface. Two studies on such systems examined the physical aging of glassy PSF alternating with a rubbery olefin block copolymer as a function of decreasing individual layer thickness using gas permeability[18] and differential scanning calorimetry (DSC).[19] No change in aging rate was observed down to layer thicknesses of 185 nm, the thinnest they measured. However, it should be noted that the forced assembly method of producing these samples results in ultrathin layers and interfaces that are not necessarily thermodynamically stable, which can limit the amount of annealing above T_g done to initiate the physical aging measurements.

Materials and Methods

For fluorescence measurements, PnBMA (**Figure 11b**) of reported molecular weight M_w = 319,200 g/mol and dispersity (Đ) of 2.58 was obtained from Scientific Polymer Products, Inc. 1-pyrenyl butyl methacrylate (aka "pyrene") (**Figure 11c**) was chemically attached to PS (**Figure 11a**) via free radical polymerization giving M_w = 582,200 g/mol and Đ = 1.58 (as measured by gel permeation chromatography). Bulk PnBMA films were spin-coated from toluene onto quartz and then annealed for 18 h at 80°C under vacuum to remove excess solvent. PS films were spin-coated from toluene onto freshly cleaved mica (providing an atomically smooth surface) and annealed for 18 h at 120°C under vacuum. The PS films were then cut into two pieces and floated onto deionized (DI) water: one piece onto a PnBMA film on quartz and the other onto silicon wafers. These films were allowed to dry before fluroescence measurements. The thicknesses of single layers on Si were measured via ellipsometry; this measurement was taken as the PS thickness in the bilayer, consistent with common fluorescence practice. The bilayer films were placed in an Instec heater within a Photon Technology International QuantaMaster fluorimeter and heated up to 120°C for 40 minutes to heal the interface and reset the sample's thermal history. The films were then cooled at

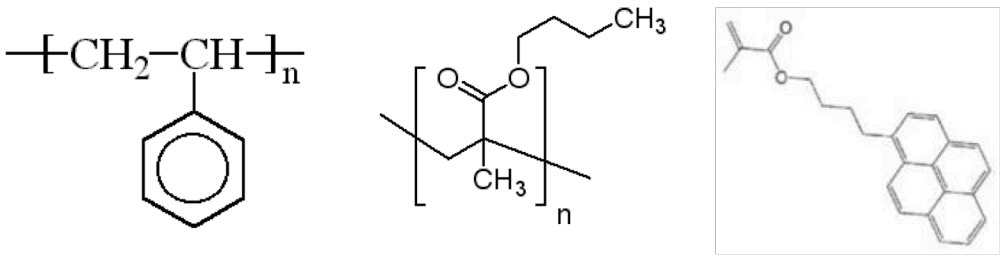

(a) (b) (c)

Figure 11. Chemical structures of (a) PS, (b) PnBMA, and (c) 1-pyrenyl butyl methacrylate ("pyrene")

1°C/minute down to 30°C while measuring the fluorescence intensity. The fluorophores were excited at a wavelength 330 nm and emission was measured at a wavelength of 379 nm for 3 s every 30 s. Data taken in our lab[25] has shown that this modified fluorescence protocol measures the same T_g for thin PS films as the method used in refs. 7, 8, 9, 12, 14.

For ellipsometry measurements, PS and PnBMA of molecular weight M_w = 934,000 g/mol and Đ = 1.14 and M_w = 319,200 g/mol and Đ = 2.58 were obtained from Polymer Source, Inc and Scientific Polymer Products, Inc, respectively. PS films were spin coated from a PS/toluene solution onto mica. PnBMA films were spin coated from toluene onto silicon wafers. PS and PnBMA films were annealed under vacuum at 125°C for ~18 h to erase thermal history and drive out excess solvent. PS films were then floated onto DI water and caught on top of PnBMA films. These bilayers were then annealed at 120°C for 30 min under vacuum in order to evaporate any remaining water, heal the PS/PnBMA interface and again erase thermal history. The bilayers were then quenched through the T_g of PS (100°C) by placing them on a room temperature aluminum block for 1 minute. The films were then transferred onto the ellipsometer (J. A. Woollam Co. Inc. M-2000 model) and held at 65°C, such that the PS layer was below its T_g (and therefore glassy) and the PnBMA was above its T_g (26°C) and therefore rubbery and in equilibrium. Samples were then given 10 minutes to fully equilibrate to that temperature. Nitrogen gas was flowed through the sample chamber at 50 cc/min throughout the aging run to prevent uptake of water by the PnBMA layer. The width of the PS/PnBMA interface was taken to be 7 nm for all bilayer measurements in accordance with the literature.[16] Data were analyzed using CompleteEASE (from J.A.

Woollam Co. Inc.) and Origin 7.5. The details of this analysis were developed specifically for this project and will be described and justified in the Results and Discussion section.

Results and Discussion

T_g of Bilayer Films as Measured by Fluorescence

Given that physical aging rate reductions in PS single layers are correlated with T_g reductions at a similar length scale (i.e. film thickness),[6] I expect that PS aging rates in the bilayer system will also correlate with the T_g of the PS layer atop PnBMA. Fluorescence measurements indicate that the PS/PnBMA bilayers exhibit much larger T_g reductions than single layer PS as shown in **Table 1**. Furthermore, these reductions occur on a significantly larger length scale. These results indicate that the PS in the bilayer may possess *two* regions of enhanced dynamics: one stemming from the free surface and another stemming from the glassy/rubbery interface.

Table 1. PS T_g as a function of PS layer thickness for single layers and PS/PnBMA bilayers. The T_g reductions in the bilayers are greater in magnitude and length scale, suggesting enhanced dynamics at both the free surface and the glassy/rubbery interface.

PS Layer Thickness	PS Single Layer T_g(°C) (estimated from ref. 12)	PS Bilayer T_g (°C)
53 nm	96	59 ± 5
75 nm	98	61 ± 2
84 nm	98	71 ±5
Bulk	100	100 (presumed)

Such an interpretation is supported by recent findings from Walczak et al.[20] who used magic-angle NMR on co-extruded PS/polycarbonate multilayers. They found that at a temperature in between the T_gs of PS and PC (i.e. when the PS is rubbery and the PC is glassy), the PC layers exhibited increased flexibility.[20] A similar interaction may be present in the PS/PnBMA system: increased flexibility and mobility in the PS layer near

the glassy/rubbery interface could allow it to remain in equilibrium at lower temperatures, resulting in larger T_g reductions as compared to single layers. Given that the bilayers exhibit *lower* T_g's in confinement as compared to single layers, I expect that the bilayers' physical aging rates will also be more greatly reduced than the single layers'.

Method of Physical Aging Rate Measurement in Bilayer Films

In order to develop a reliable method for measuring the physical aging rate of PS in the bilayer morphology with ellipsometry, I first conducted simple control measurements. I used the streamlined ellipsometry procedure[5] described earlier, taking one measurement each minute, averaging over 40 seconds every minute for a 6 hour period. Each layer in the measurements were fit with a layer film thickness and the first two terms of a Cauchy model, shown below:

$$n_i(\lambda) = A_i + \frac{B_i}{\lambda^2} \tag{7}$$

I first measured the behavior of ~500 nm thick PnBMA single layers (for which we expect bulk properties) at 65°C (the standard aging temperature for all subsequent measurements), well above the polymer's T_g and therefore in equilibrium. Early measurements showed increases in the thickness *and* index of refraction of the film, indicating an increase in mass over the course of the aging run. This was believed to be the result of water uptake by the PnBMA. To avoid this, high-purity N_2 gas was flowed through the sample chamber for all subsequent measurements at 50 cc/min, which effectively established a dry atmosphere. The left side of **Figure 12** shows the thickness of a 523 nm thick single layer of PnBMA, fitting for film thickness and Cauchy

parameters A and B. As expected, no change in layer thickness or index of refraction was observed during the aging period.

Several control measurements showed that the PnBMA layer thickness can take ~ 30 min to stabilize once placed on the ellipsometer hot stage. In order to be certain that the rubbery PnBMA layer is stable at the beginning of the aging period, the volumetric aging rates were calculated by cropping the first 60 minutes of data and normalizing the data to values at 60 min. As all methods of analysis (detailed below) rely on the initial thicknesses of various layers within the film for normalization, it is useful to explicitly define what is meant by the term "initial." The initial thickness $h_{0,i}$ of a polymer layer 'i' is taken as a 10-minute average of layer thickness centered about the 60-minute time mark, which is the beginning of the aging time in my analysis as described above. Averaging over a 10-minute period helps to account for small fluctuations in layer thickness due to noise from the instrument. The term "initial" will also sometimes refer to initial values of the Cauchy parameters A and B. In this case, the values are also 10-minute averages centered about the 60-minute time mark.

The right side of **Figure 12** shows the total thickness of a bilayer film comprising a 525 nm PnBMA layer and a 415 nm PS layer, fitting film thickness and Cauchy parameters A and B for each layer. This particular sample will be very useful in illustrating various methods of analysis and will be referred to as "Bilayer 1" for the remainder of this work. The total thickness decreased linearly with the logarithm of time, in accordance with expected physical aging behavior. The vertical scale intervals are identical for both graphs in **Figure 12** for convenient direct comparison. Given that the thickness of single layer PnBMA *does not* change over time while the thickness of a

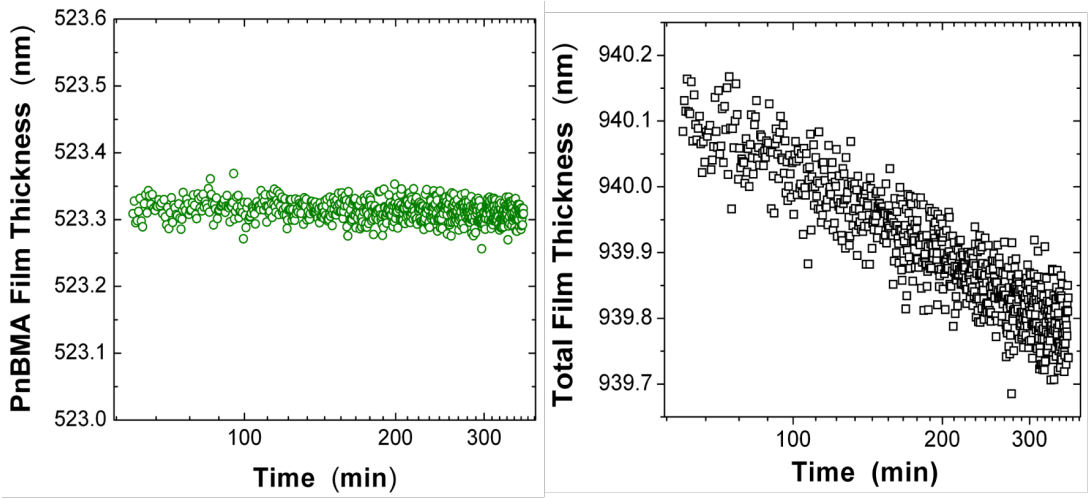

Figure 12. Film thickness over a 6 hour period for a 523 nm single layer of PnBMA (left) and a PS/ PnBMA bilayer comprising 525 nm of PnBMA and 415 nm of PS (right) at 65°C. As expected, the PnBMA single layer's properties do not vary over time (since it is above its T_g) while the bilayer's thickness decreases with the logarithm of time. Given these two results, we can safely assume that all thickness decreases in the bilayer, and therefore all physical aging, comes from the PS layer.

bilayer with the same thickness of PnBMA *does* vary, we can safely assume that all thickness changes, and therefore all physical aging, comes from the PS layer.

With this assumption in hand, I analyzed the data from the bilayers in three different ways to determine the aging rate of the PS layer in the bilayer system, which I refer to as the "bilayer aging rate." First, I fit the thickness and the A and B parameters for each of the polymer layers – 6 parameters in all − and examined the total thickness (obtained by summing the fitted thickness of each layer and the interfacial width). The bilayer aging rate in terms of total film thickness is given by **Equation 8**:

$$\beta = -\frac{1}{h_{0,PS}}\left(\frac{\partial h_{total}}{\partial \log t_a}\right) \tag{8}$$

where h_{total} is the total thickness of the bilayer, $h_{0,PS}$ is the initial PS layer thickness,* and t_a is the aging time. Inherent in this equation is the previously justified assumption that the change in total film thickness is the same as the change in PS layer thickness, which makes it mathematically equivalent to the equation used by Baker et al.[5] Rearranging **Equation 8** and integrating, we can see that the total film thickness as a function of time is given by **Equation 9**:

$$h_{Total} = h_{0,total} - h_{0,PS}\beta(\log t_a) \tag{9}$$

where $h_{0,Total}$ is the initial total film thickness. The best fit of **Equation 9** to the total thickness of Bilayer 1, shown in the top left panel of **Figure 13** along with total thickness measurements, yields a bilayer aging rate of $\beta = 10.7 \times 10^{-4}$. This analysis protocol will be referred to as "Method 1" in the future.

In the second method of analysis, I again fit all 6 ellipsometry parameters but focused on the individual thicknesses of the PS and PnBMA layers. The thickness of the PnBMA layer in Bilayer 1 over time is shown in the top middle panel of **Figure 13** and the thickness of the PS layer in Bilayer 1 (normalized by the initial PS layer thickness) is shown in the top right panel of **Figure 13**. The bilayer aging rate is now essentially the same equation used by Baker et al.[5] shown below:

$$\beta = -\frac{1}{h_{0,PS}}\left(\frac{\partial h_{PS}}{\partial \log t_a}\right) \tag{10}$$

* This value was found to be within 3% of the thickness of the PS layer before it was floated onto the PnBMA which is the reported PS thickness in bilayer T_g measurements. Therefore, the T_g data and physical aging rate data can be easily compared.

where h_{PS} is the thickness of the PS layer. Rearranging and integrating **Equation 10** in the same manner as **Equation 8**, we find that the normalized PS thickness as a function of aging time is given by:

$$\frac{h_{PS}}{h_{0,PS}} = 1 - \beta \log t_a \tag{11}$$

This method does not rely on the assumption that the properties of the PnBMA remain constant throughout the aging period as it allows both layers to vary freely, but only focuses on the PS layer. However, the top middle panel of **Figure 13** does serve to further validate this assumption. The best fit of **Equation 11** for the data from Bilayer 1 is shown by the red line in the top right panel of **Figure 13** and corresponds to a bilayer aging rate of $\beta = 9.8 \times 10^{-4}$. This analysis protocol will be termed "Method 2" for the remainder to this work.

The third method of analysis I used relies heavily on the assumption that the PnBMA layer's properties do not vary over the course of the aging period. Instead of fitting six parameters, I fit only three – thickness, A, and B for the PS layer – setting the thickness and A and B parameters of the PnBMA layer constant at their initial values (as obtained from the fitting done for the second method of analysis). The thickness of the PnBMA layer in Bilayer 1 under this approximation is shown in the bottom middle panel of **Figure 13** while the PS layer thickness of Bilayer 1 (normalized by the initial PS layer thickness) is shown in the bottom right panel of **Figure 13**. Again, the bilayer aging rate is given by **Equation 4** and the normalized PS layer thickness over time is therefore given by **Equation 11**. The best fit of **Equation 11** is shown by the red line in the

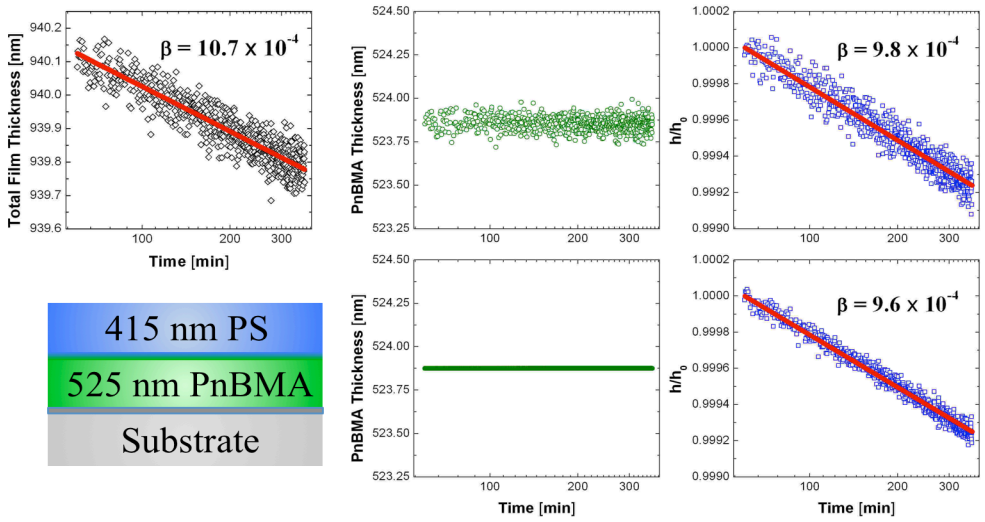

Figure 13. Physical aging rates of PS in Bilayer 1 as determined by various methods of analysis. The total film thickness determined by fitting layer thickness and A and B Cauchy parameters for each layer is shown in the top left graph, with the red line corresponding to the best fit of **Equation 9**. The top middle panel shows the PnBMA thickness when fitting all 6 parameters and the top right graph shows the normalized PS layer thickness, with the red line corresponding to the best fit of **Equation 11**. The PnBMA thickness of Bilayer 1 when only fitting the PS layers' parameters is shown in the bottom middle graph and the normalized PS layer thickness is shown in the bottom right, with the red line again corresponding to the best fit of **Equation 11**. The final method produces considerably less noise than the first two and is found to be the most reliable when the PS layer becomes thin.

bottom right panel of **Figure 13** and results in a bilayer aging rate of $\beta = 9.6 \times 10^{-4}$. This analysis protocol will be referred to as "Method 3."

Performing these three methods of analysis on bilayers with PS thickness greater than 400 nm, I determined a bulk aging rate and experimental error for each method (taken to be one standard deviation). The bulk aging rates and experimental errors for Method 1, Method 2, and Method 3 were found to be 9.6 (±1.2) × 10^{-4}, 9.3 (±0.5) ×10^{-4}, and 9.5 (±0.3) × 10^{-4}, respectively. These values are all well within error of each other in the regime of bulk PS aging behavior. However, there is significantly less noise in the data used for Method 3 as compared to Method 1 and Method 2, which may yield more reproducible results. Since Method 1 is not focused on the fitted thickness of the PS layer, but rather the total thickness of the film, it may not be expected to agree

quantitatively with Method 2 and Method 3. However, the total fitted thickness of the film would provide a better measure of the raw data than the individual layer thicknesses because several combinations of individual layer thicknesses can result in the same total thickness, potentially allowing for greater variability in the individual thicknesses. Therefore, qualitative agreement between Method 1 and the other methods across a variety of PS layer thicknesses will be a good indicator of each method's validity.

Figure 14 shows the bilayer aging rate as a function of initial PS layer thickness as determined by the various methods of analysis. Each data point is an average of 2-4 nominally identical samples and error bars are one standard deviation. Method 1 (blue squares) and Method 3 (green diamonds) are in good qualitative agreement (aside from the data point at ~135 nm, which is only an average of two samples). In general, Method

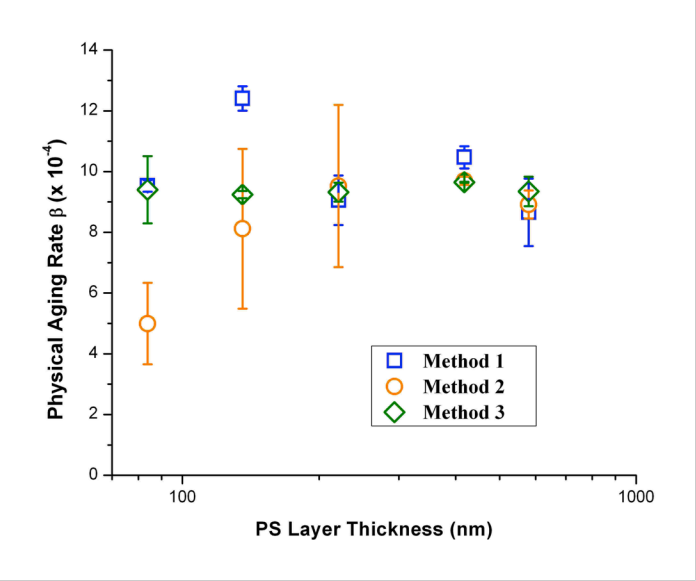

Figure 14. Bilayer aging rate versus initial PS layer thickness comparing the different methods of analysis. Method 1 and Method 3 agree qualitatively and have relatively small error bars, indicating reliable and reproducible measurements. Method 2 shows large variations across nominally identical samples, especially for thin PS layers. In many cases, the fitted PnBMA layer thickness in Method 2 was found to decrease significantly over time (an unphysical result) which indicates that the PnBMA dominates the signal and the ellipsometry software attributes a significant portion of the decrease in total film thickness to the rubbery layer, distorting the aging rate of the PS layer.

3 results in the least variation in aging rate across nominally identical samples (smallest error bars) and the least variation in aging rate across those PS layer thicknesses in which we expect bulk aging rates (>200 nm). Method 2 results in very large scatter across nominally identical samples and does not agree qualitatively with Method 1 or Method 3. While this method seems to indicate a decrease in bilayer aging rate with decreasing PS layer thickness, when this occurs the PnBMA layers showed significant reductions in thickness over time − a nonphysical result inconsistent with the control measurements done on single layer PnBMA films. When the PS layer becomes thin relative to the PnBMA layer thickness, the ellipsometery signal can become dominated by the PnBMA layer, limiting the ability to reliably identify the much thinner PS layer separately. Thus, the ellipsometry software fits the data with more and more of the decrease in total film thickness being attributed to the PnBMA layer. Because of these fitting concerns, it was decided to fix the PnBMA layer thickness at the initial thickness measured −the Method 3 analysis. This method is felt to be the most reliable at identifying a meaningful aging rate for the thinner PS layers, and yields the most reproducible aging rates. All further discussions in this work are based on the bilayer aging rate as determined by a best fit of **Equation 11** to data fitted by the ellipsometry software under the approximation that all PnBMA layer properties remain constant throughout the aging period (Method 3).

Physical Aging Rate of Bilayer Films with Varying Layer Thickness

Having established a consistent and appropriate method for measuring and analyzing the aging of the PS layer, I then conducted a series of measurements to determine the impact of PnBMA layer thickness on the bilayer aging rate. **Figure 15** shows the normalized thickness of three ~220 nm PS layers on top of PnBMA layers of

thickness 1300 nm (purple data), 500 nm (green data) and 45 nm (orange data). No change in bilayer aging rate was observed. The aging rates for all three data sets shown average to $\beta = 9.3\ (\pm 0.3) \times 10^{-4}$. Given that the bilayer aging rate is independent of PnBMA layer thickness down to 45 nm, I used 500 nm PnBMA layers for all subsequent measurements since it is a convenient sample thickness for the ellipsometer and is well within the range of bulk behavior, thus guaranteeing elimination of substrate effects on the PS layer.

I then collected data on the bilayer aging rate varying the initial PS layer thickness. **Figure 16** shows the normalized thickness of three selected initial PS layer thicknesses (one sample each) on top of ~500 nm layers of PnBMA over the course of the 6 hour aging period. The blue data correspond to an initial PS layer thickness of 580 nm,

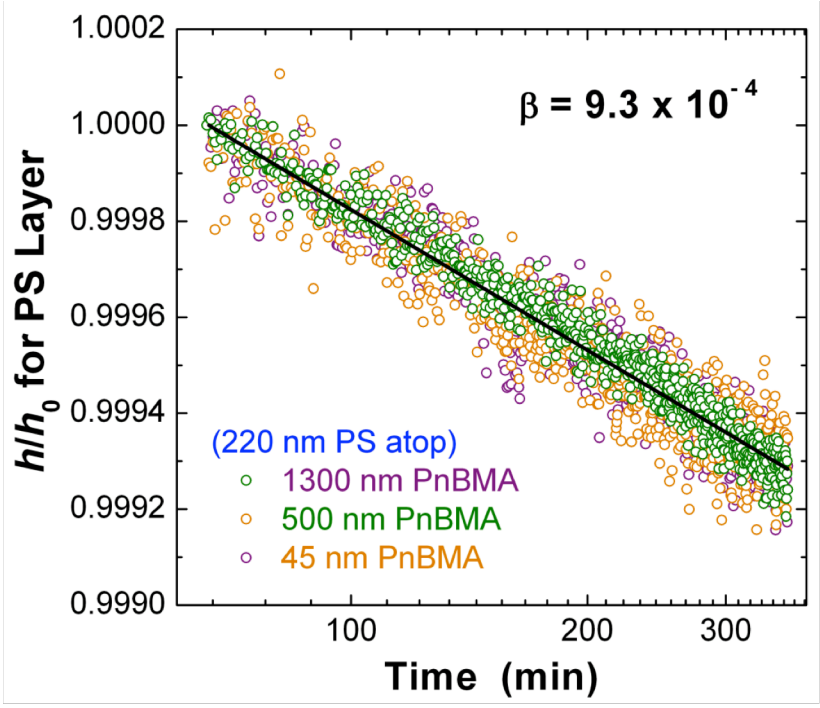

Figure 15. Normalized PS layer thickness for ~220 nm thick layers of PS on top of PnBMA layers of thickness 1300 nm (purple), 500 nm (green) and 45 nm (orange). The black line is a best fit of **Equation 11** for the green data. The average aging rate of the samples shown is $\beta = 9.3\ (\pm 0.3) \times 10^{-4}$.

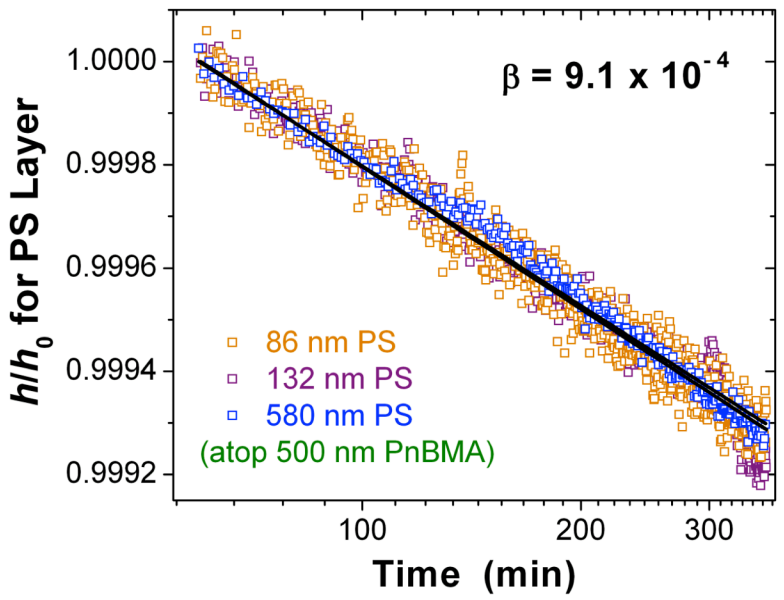

Figure 16. Normalized PS layer thickness for PS layers of initial thickness 580 nm (blue), 132 nm (purple) and 86 nm (orange) on top of PnBMA layers of thickness 500 nm. The black lines are best fits of **Equation 11** for each of the three data sets. The average aging rate of the samples shown is $\beta = 9.1\ (\pm 0.1) \times 10^{-4}$.

the purple to an initial PS layer thickness of 132 nm, and the orange to an initial PS layer thickness of 86 nm. The average aging rate of the three samples shown is $\beta = 9.1\ (\pm 0.1) \times 10^{-4}$. This is an unexpected result. Despite large T_g reductions in PS/PnBMA bilayer films, we observe *no change* in physical aging rate of PS supported on bulk PnBMA as the initial PS thickness is decreased. Even down to PS layer thicknesses of 86 nm, where T_g is reduced to within 5°C of the aging temperature we observe *no reduction* in the physical aging rate. This result stands in direct contrast to Pye et al.'s data for single layer PS, where physical aging rate reductions accompany the T_g reductions seen at comparable film thicknesses.[6] For example, they found that at an aging temperature of 65°C, a 29 nm thick single layer film of PS showed a decrease in physical aging rate of $\Delta\beta = -3.1 \times 10^{-4}$ relative to bulk, when the film had an average T_g reduction of -10°C. In

contrast, I have found that despite an average T_g reduction of -30°C for an 84 nm thick layer of PS on top of bulk PnBMA, there is *no* corresponding aging rate reduction.

To better illustrate this result, **Figure 17** plots the bilayer aging rate (blue squares) and the single layer PS aging rate (grey circles) as a function of initial PS layer thickness. The open symbols correspond to PS layers with no observed T_g reductions, i.e. films that

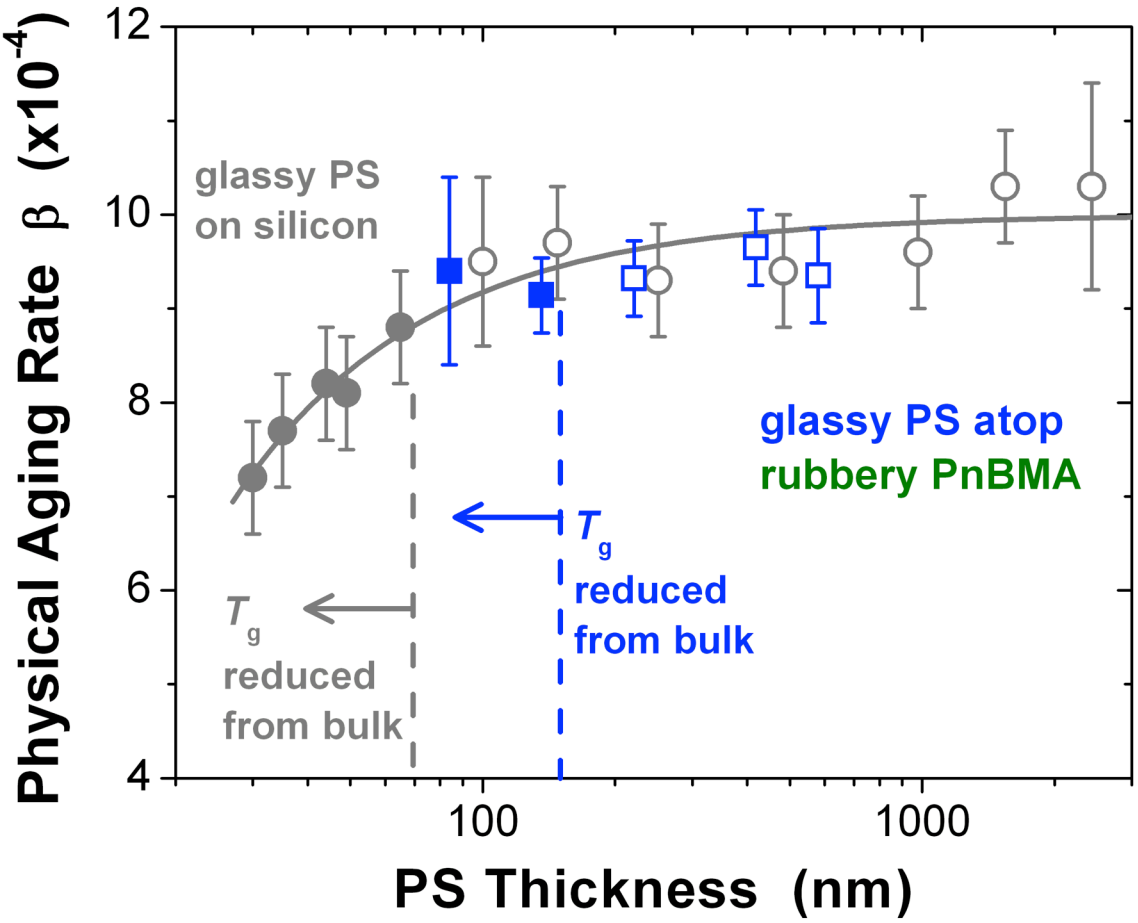

Figure 17. Single PS layers (gray circles) exhibit reduced aging rates in films with reduced T_g (solid circles) and bulk aging rates in films showing bulk T_g (open circles). [Data taken from ref. 6]. Similar to the PS single layers, the PS/PnBMA bilayers (blue squares) also exhibit bulk aging rates when no T_g reductions are present (open squares). However, in contrast to single layers, the bilayers showed no reductions in aging rate even when T_g is significantly reduced from bulk (closed squares). The smallest single layer thickness measured (29 nm) shows T_g reductions of -10°C and a significantly reduced aging rate. However, the 84 nm and 136 nm thick PS layers in the bilayer system show T_g reductions of -30°C and -10°C, yet still have no change in physical aging rate. This leads me to conclude that there must be some competing effect at the interface. Blue data points are averages of 2-4 samples; gray data points are averages from 2-6 samples. The gray curve is the best fit to the equation $\beta = \beta_{Bulk}(1\text{-}A/h)$ where β is the single layer PS physical aging rate, β_{Bulk} is the bulk PS aging rate, h is the PS thickness, and A is the thickness of the liquid-like surface layer (see Background section and ref. 6 for analysis).

have T_gs equivalent to bulk T_g, while the closed symbols correspond to PS layers *with* T_g reductions. For the single layer films, the decrease in aging rate occurs at approximately the same thickness at which T_g reductions begin (indicated by the gray dashed vertical line). In contrast, for the bilayer films, no decrease in aging rate is observed well below the PS layer thickness at which T_g reductions occur, indicated by the blue dashed vertical line).

These results, while unexpected, are not necessarily inconsistent with previous observations in related systems. As described earlier, other studies have used gas permeability[18] and DSC[19] to show that alternating glassy/rubbery multilayers show no change in aging rate as the glassy layer thickness is decreased.

We can try to understand these results by a simple approximation considering the PS layer as a combination of a free surface layer, a bulk middle layer, and the glassy/rubbery interface. One might initially guess that the average aging rate by ellipsometry and the average T_g measured by fluorescence might be a simple average of local aging rates and local T_gs of these three regions. Following Pye et al,[6] I could assume that the middle layer has no reduced T_g and undergoes bulk aging while the free surface has a greatly reduced T_g and undergoes no aging. To estimate the T_g of the interface layer in my simple model, I use the Fox-Flory Equation for T_g of polymer blends:[21]

$$\frac{1}{T_{g,Blend}} = \frac{\phi_1}{T_{g,1}} + \frac{\phi_2}{T_{g,2}} \tag{12}$$

where $T_{g,Blend}$ is the T_g of the blend, $T_{g,1}$ and $T_{g,2}$ are the T_gs of the two different polymers and ϕ_1 and ϕ_2 are the volume fractions of the two polymers. While this equation was developed to describe miscible polymer blends, and PS and PnBMA are weakly

immiscible, this equation is a reasonable first approximation for the local T_g of the interface region where the polymers are locally mixed. Assuming equal volume fractions of PS and PnBMA, I determined that the interface should have a local T_g of approximately 333 K or 60°C. For the measurements shown in **Figure 17**, the aging temperature was held constant at 65°C, such that the glassy/rubbery interface would be above this predicted local T_g and would therefore experience no aging. The average of these estimated aging rates of the three domains can only result in a value that is *lower* than bulk PS (since it includes one layer with bulk aging rate and two layers with zero aging), which is inconsistent with the observed measurements. Therefore, I propose that the lack of an aging rate reduction in the bilayers may be due to some yet unknown mechanism that acts to locally increase the aging rate at the glassy/rubbery interface counteracting the assumed decrease in aging rate that likely occurs at the free surface.

I identify two possibilities, yet at present have no evidence to suggest one over the other and consequently attach no weight to either one. First, a free volume type argument may be appropriate. PnBMA is soft and flexible and therefore could allow for denser chain segment packing at the PS interface. Indeed, it has been shown that the interfaces of immiscible polymers can be denser than either polymer individually.[4] Changes in chain segment configuration may affect mobility in the surrounding region, leading to differences in local aging rate. This could be tested experimentally by conducting identical aging measurements on a PS/rubbery bilayer in which the rubbery polymer has very different side groups (e.g. polybutadiene). However, great care must be taken in choosing an appropriate polymer that closely resembles PnBMA both in T_g and in its

interaction with PS as these would affect the local T_g of the glassy/rubbery interface as well as the interfacial width.

Second, an increased aging rate at the interface could result from increased local stresses. Recent work from the Roth lab has shown that stress during the thermal quench can significantly impact the physical aging rate of PS.[22,23] During the thermal quench, a film supported on silicon experiences a very large in plane stress (~12 MPa) due to thermal expansion mismatch between the polymer film and the underlying substrate.[22] These stresses may be altered by the presence of the interface. The measurements presented in this thesis involving varying the layer thickness of PnBMA (**Figure 15**) were done in part to test if the stresses originating from the substrate were being transmitted to the entire film; a difference in aging rate would indicate a difference in stress. The physical aging rate of thick (~220 nm) PS layers atop PnBMA is found to be consistent with that of bulk single layer PS films suggesting that the same stress from the substrate is being transmitted to the glassy PS layer through the rubbery PnBMA. However, it is entirely possible that local stress at the glassy/rubbery interface and surrounding region may be different leading to a different and possibly increased "aging" rate that may actually be stress relaxation at the interface. Again, these are merely speculations and further studies and analysis of the polymer-polymer interface are required.

Bilayer Aging Rate vs. Aging Temperature

In an effort to further characterize the behavior of the PS/PnBMA bilayers, I measured the bilayer aging rate of 55 nm glassy PS layers atop 500 nm rubbery PnBMA layers as a function of aging temperature. The results are shown by the orange symbols

in **Figure 18** with the black curve corresponding to a simple quadratic fit of the data to guide the eye. The bilayer aging rate increases continuously up to the point where the average reduced T_g of the glassy PS layer (59°C for this system) is nearly equal to the aging temperature. Again, this result stands in contrast to the observed behavior of bulk 2400 nm PS single layer films and confined 29 nm thick single layer PS films, reproduced from ref. 6 (**Figure 9**) onto **Figure 18**[*]. As yet, I cannot suggest an explanation for this behavior, but it is quite clear that the glassy/rubbery interface perturbs thin PS films in a qualitatively and quantitatively significant manner.

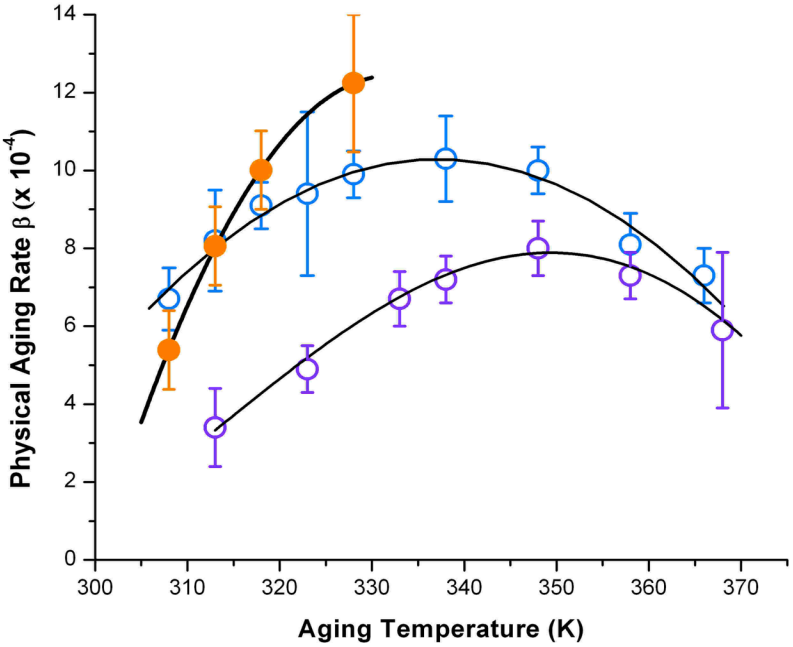

Figure 18. Physical aging rate as a function of aging temperature for 55 nm thick PS layers atop bulk 500 nm thick PnBMA (orange data, fit with a 2nd order polynomial to guide the eye). Data for single layer PS films also shown for comparison: ~2400 nm bulk PS (blue data, fit with 2nd order polynomial by Pye et al.[6]) and 29 nm thick PS (purple data, fit by **Equation 4**) on silicon [Data taken from ref. 6]. Surprisingly, unlike single layer PS films, bilayers do not show a maximum in aging rate below the average reduced T_g of the PS layer (59°C).

[*]Note that the single layer data from ref. 6 was normalized at 10 minutes of aging time, while the bilayer data was normalized at 60 minutes. This would not affect qualitative trends, but may account for some small qualitative differences.

Conclusions and Future Directions

Expanding on previous ellipsometry techniques,[5] I developed a method to reliably measure the physical aging rate of glassy PS atop rubbery PnBMA by approximating the properties of the rubbery layer as constant. Extensive control measurements and analysis were performed to verify this approximation. I then used this technique to measure the physical aging rate of glassy PS in the bilayer system and found that despite large T_g reductions, there was no observed change in physical aging rate, suggesting the presence of some competing effect at the glassy/rubbery interface. I also used fluorescence spectroscopy to measure the T_g of glassy PS atop rubbery PnBMA and found that the T_g's of thin PS films are more greatly reduced in the bilayer system than for single layer PS films.

To further characterize the effect of the glassy/rubbery interface, I propose a few possibilities for future research in order to determine a characteristic length scale for the interfacial effect. To obtain a measure of this length scale, we can follow an analysis similar to Pye et al.[6] and construct a model to account for two exponential gradients in dynamics: one from the free surface and another from the interface, each with their own length scale. Whereas Pye et al.[6] could safely assume that the physical aging rate near the substrate is essentially bulk (based on data from Ellison and Torkelson[7]), no such assumption can be made concerning the magnitude of the effect stemming from the interface. Therefore, this double-gradient model involves both magnitude and length scale, two non-independent fitting parameters (i.e. the same average aging rate could be obtained from a large effect with a short range or a small effect with a long range), but only one data set, so another kind of measurement is required. For this, I suggest a

reverse bilayer, rubbery PnBMA atop glassy PS, in which the magnitude and length scale of the interfacial effect are presumably the same as in the traditional bilayer. In this system, we could follow Pye et al.[6] and assume bulk aging at the substrate. Therefore, between the these experimental morphologies, we have two fitting parameters and two unique data sets, such that simultaneous modeling of both of these systems would allow us to effectively probe both the magnitude and the length scale of the interfacial effect.

Furthermore, studies on other PS/rubbery bilayers will also serve to determine the effects of rubbery layer T_g, flexibility, side group size, and specific polymer-polymer interactions on the physical aging rate of PS. It also may be possible to directly measure the stress at the PS/PnBMA interface. Certain compounds undergo bond scission and become fluorescent when subjected to macroscopic stresses.[24] PS layers could be doped with such compounds and then quenched in a controlled manner while measuring the fluorescence signal. Measurements of PS single layers and PS/PnBMA bilayers could be compared to determine relative differences in stress in the two systems.

The glass transition and physical aging are still poorly-understood phenomena. How and why specific interfaces affect the physical aging and T_g of glassy polymers is still an open question in the field. In this work I determined some of the "how" and speculated about some of the "why." My results are unexpected and help lay the groundwork for future investigations into the nature of the glass transition and physical aging in highly applicable glassy/rubbery systems.

References

(1) Ryan C, Christenson CW, Valle B, Saini A, Lott J, Johnson J, Schiraldi D, Weder C, Baer E, Singer KD, Shan J. *Advanced Materials* **2012**, *24,* 5222-5226

(2) Rowe BW, Freeman BD, Paul DR. *Polymer* **2009**, *50*, 5565-5575

(3) Liu RYF, Jin Y, Hiltner A, Baer E. *Macromol. Rapid Commun.* **2003**, *24*, 943-948

(4) Liu RYF, Bernal-Lara TE, Hiltner A, Baer E. *Macromolecules* **2004**, *37*, 6972-6979

(5) Baker EA, Rittigstein P, Torkelson JM, Roth CB. *Journal of Polymer Science: Part B: Polymer Physics*, **2009**, *47*, 2509-2519

(6) Pye JE, Rohald KA, Baker EA, Roth CB. *Macromolecules* **2010**, *43*, 8296-8303

(7) Ellison CJ, Torkelson JM. *Nature Materials*, **2003**, *2*, 695-700

(8) Roth CB, McNerny KL, Jager WF, Torkelson JM. *Macromolecules* **2007**, *40*, 2568-2574

(9) Roth CB, Torkelson JM. *Macromolecules* **2007**, *40*, 3328-3336

(10) Tompkins, HG. *A User's Guide to Ellipsometry*. Mineola: Dover Publications, Inc. 1993. Print. Pg. 17

(11) Keddie JL, Jones RAL, Cory RA. *Europhysics Letters* **1994**, *27*, 59-64

(12) Ellison CJ, Mundra MK, Torkelson JM. *Macromolecules* **2005**, *38*, 1767-1778

(13) Keddie JL, Jones RAL, Cory RA. *Faraday Discuss.* **1994**, *98*, 219-230

(14) Priestley RD, Mundra MK, Barnett NJ, Broadbelt LJ, Torkelson JM. *Australian Journal of Chemistry* **2007**, *60*, 765-771

(15) Forrest JA, Mattsson J. *Phys. Rev. E* **2000**, *61*, R53– R56

(16) Siqueria DF, Schubert DW, Erb V, Stamm M, Amato JP. *Colloid Polymer Sci.* **1995**, *273*, 1041-1048

(17) Tant MR, Wilkes GL. *Polymer Engineeering and Science* **1981**, *21,* 325-330

(18) Murphy TM, Langhe DS, Baer E, Freeman BD, Paul DR. *Polymer* **2011**, *52*, 6117-6125

(19) Murphy TM, Langhe DS, Ponting M, Baer E, Freeman BD, Paul DR., *Polymer* **2012***, 53,* 4002-4009

(20) Walczak M, Ciesielski W, Galeski A, Portzebowski MJ, Regnier G, Hiltner A, Baer E. *Journal of App. Polym. Sci.* **2012**, *125*, 4267-4274

(21) Sperling LH. *Introduction to Physical Polymer Science: 4th Edition*. Hoboken: John Wiley & Sons, Inc. 2006. Print. Pg. 401

(22) Gray LAG, Yoon SW, Pahner WA, Davidheiser JE, Roth CB. *Macromolecules*, **2012**, *45*, 1701-1709

(23) Gray LAG, Roth CB. *Submitted*.

(24) Black AL, Lenhardt JM, Craig SL. *Journal of Materials Chemistry* **2011**, *21*, 1655-1663

(25) Baglay, R. "Probing the Gradient in Glass Transition Temperatures Across a Glassy/Rubbery Polymer-Polymer Interface." *Rotation Report,* **2012**